Various approximations made in augmented-plane-wave calculations

N. C. Bacalis, K. Blathras, and P. Thomaides
Research Center of Crete, Institute of Electronic Structure and Laser, P.O. Box 527, Heraklion, Crete 711 10, Greece

D. A. Papaconstantopoulos
Metal Physics Branch, Naval Research Laboratory, Washington D.C. 20375
(Received 22 April 1985)

The effects of various approximations used in performing augmented-plane-wave calculations were studied for elements of the fifth and sixth columns of the Periodic Table, namely V, Nb, Ta, Cr, Mo, and W. Two kinds of approximations have been checked: (i) variation of the number of k points used to iterate to self-consistency, and (ii) approximations for the treatment of the core states. In addition a comparison between relativistic and nonrelativistic calculations is made, and an approximate method of calculating the spin-orbit splitting is given.

I. INTRODUCTION

Calculations using the augmented-plane-wave[1,2] (APW) method have been performed throughout the years with certain approximations. The effects of these approximations are more or less qualitatively known, but no systematic study of their differences has been done. In this work we have investigated these approximations for the elements of the fifth and sixth columns of the Periodic Table, i.e., for V, Nb, Ta, Cr, Mo, and W, and drawn conclusions about their sufficiency and other aspects of their results. The approximations we have studied are the following: (1) the inclusion of relativistic effects without the spin-orbit interaction, (2) the effect of the spin-orbit interaction, (3) the effect on self-consistency of using different k-point meshes, (4) the "soft-core" approximation versus the "frozen-core" approximation, and (5) the effect of treating the so-called "semi-core" states as bands.

II. METHOD OF CALCULATION AND APPROXIMATIONS

The above-mentioned elements crystallize in the bcc structure. The lattice constants were taken from Wyckoff.[3] All the calculations were performed in the muffin-tin approximation, self-consistently, using a standard symmetrized APW code without linearization. For a general k point, 50 plane waves were used, which corresponds to a level of convergence that is better than 10^{-4} Ry. The crystal potential was calculated on a doubling linear mesh of 218 values inside the muffin-tin sphere. The exchange potential was calculated using the local-density theory of Hedin and Lundqvist[4] (HL), and for comparison one calculation was made by the $X\alpha$ method. The Fermi energies and the densities of states were calculated by the tetrahedral method,[5] using as input the energies of a 55-k-point mesh in a $\frac{1}{48}$th section of the first Brillouin zone. Recently, a possible misapplication of the tetrahedron method has been pointed out[5] which leads to wrong weighting of certain symmetry points. Our calculations do not suffer from this problem.

First we studied the relativistic effects by performing both nonrelativistic calculations, i.e., solving the Schrödinger equation, and relativistic calculations, i.e., solving the Dirac equation in the crystal neglecting spin-orbit coupling. All the other comparisons in this work were made using the results of relativistic calculations. Three kinds of approximations were used in performing the self-consistent calculations: the "soft-core," the "frozen-core," and the "semicore" approximations as described below.

The radial charge density $\sigma(r)$ was found from the expression

$$\sigma(r)=\sum_{n,l}^{\text{core}} P_{nl}^2(r)+\sum_{n,k}\sigma_{n,k}(r)\equiv\sigma_{\text{core}}+\sigma_{\text{val}}\ , \tag{1}$$

and was used to solve the Poisson's equation in each iteration to determine the Coulomb potential, and in the Hedin-Lundqvist formula to find the exchange-correlation potential.[4] In Eq. (1), σ_{core} is the charge density of the core electrons as given by an atomic calculation. In the soft-core approximation, σ_{core} was recalculated in each iteration, while in the frozen-core approximation it was kept constant. In both cases the core was determined by the configuration of the nearest lower noble element. In the semicore approximation the core was reduced to the nearest fully occupied level, labeled by principal quantum number n. For example, in Nb the levels $4s$ and $4p$ are treated as bands in the semicore approximation. On the other hand, σ_{val} [in Eq. (1)] was formed from the contributions of the occupied bands above the core; σ_{val} was recalculated in each iteration by the APW program.

In the soft-core approximation, σ_{val} was computed from the wave functions of a set of points in $\frac{1}{48}$th of the first Brillouin zone, properly weighted in order to take into account the symmetry within the zone. Three different sets were used of 5 k points, 14 k points, and 55 k points.

For the calculation of the density of states (DOS), the 14-k-point self-consistent crystal potential was used to generate energies for 55 k points, and an interpolation

TABLE I. Comparison between iterating with 14 k points and 55 k points for niobium.

	14 k points E (Ry)	Δ_E (mRy)	55 k points E (Ry)
Γ_1	−0.470 41	0.3	−0.470 13
H_{12}	−0.324 29	0.1	−0.324 16
N_1	−0.310 66	0.2	−0.310 50
N_2	−0.150 03	0.1	−0.149 96
P_4	−0.111 92	0.1	−0.111 80
Γ'_{25}	0.000 00	0.0	0.000 00
N'_1	0.131 13	0.3	0.131 39
Γ_{12}	0.189 45	0.0	0.189 45
N_1	0.202 97	0.0	0.202 95

with the tetrahedral method was then performed. We also investigate the effect on the DOS when a 285-k-point mesh was generated by the APW calculation.

III. RESULTS AND DISCUSSION

Tables I—VI show the energies at the high-symmetry k points Γ, N, P, and H for the elements we studied. For common comparison the zero has been put at the energy of the Γ'_{25} state. In each table, the element and the approximation made is clearly shown. For each element, three columns of numbers are displayed (except in Table II, where there are five columns). The left column for each element shows the energies, in rydbergs, from the relativistic soft-core approximation, with 14 k points. In the third (fifth for Table II) column for each element, the energies of another approximation are shown, and to the left of this column the differences (in mRy) between the relevant approximation and the soft-core approximation are displayed. Tables III—V also show the s-d separation ($H'_{25}-\Gamma_1$ and $\Gamma_1-\Gamma'_{25}$), the d-band width $H'_{25}-H_{12}$, and the s-p bandwidth $N'_1-\Gamma_1$ for each case. The Fermi energies, calculated by the tetrahedral method, are also shown, along with the occupied bandwidths ($E_1-\Gamma_1$ and $E_F-\Gamma_{12}$) and the density of states at the Fermi level. In all the calculations described below, we used the HL prescription for exchange and correlation. For Mo, we performed one extra calculation using the $X\alpha$ coefficient for the exchange.[6] A comparison between this calculation and the HL one showed a maximum deviation of 2.3 mRy for the H'_{25} state and much smaller differences for the other states. We have therefore concluded that the $X\alpha$ method for treating exchange and correlation is nearly equivalent to that of HL.

A. Comparison between the various k-point meshes

We compared self-consistent calculations in which the iterations were carried out for three different k-point meshes, i.e., the uniform grids of 5, 14, and 55 k points. This comparison was performed for Nb and Ta, shown in Tables I and II. As we can see from these tables, iterating with 55 k points introduces changes of 0.2—1.3 mRy from the energies found in the calculations with the 14 k-point mesh, whereas in going from 5 k points to 14 k points the differences are 1—10 mRy. The most affected states are the s-like Γ_1 state and the p-like N'_1 state for both Nb and Ta, and generally for Nb the differences are smaller than for Ta. Since the differences between the 14-k- and the 55-k-point meshes are within the accuracy of the APW method, we conclude that the 14-k-point mesh is certainly adequate for a well-converged calculation. However, neither the 14- nor the 55-k-point meshes are sufficient input to the tetrahedral method for the evaluation of the DOS. We found that in order to obtain the DOS with high accuracy, one needs the first-principles energies on a mesh of 285 k points in the irreducible zone.

B. Relativistic effects

We compared self-consistent (SC) calculations which included the mass-velocity and Darwin relativistic corrections to nonrelativistic SC calculations. Because Ta and W are heavy atoms and the nonrelativistic results for them are expected to be inaccurate, we performed this comparison only for V, Nb, Cr, and Mo. The relativistic effects introduce differences which are, on the average, 1—30 mRy for the lighter elements V and Cr, and 3—80 mRy for the heavier Nb and Mo. In Table III, as an example, we summarize our results for Cr and Mo. The main difference between nonrelativistic and relativistic calculations (RC's) is that in the RC's the bands become wider and deeper in energy. This can be seen from Fig. 1, where the energy bands of Mo are shown from the relativistic (a) and the nonrelativistic (b) calculations. The s-d

TABLE II. Comparison between iterating with 14 k points, 5 k points, and 55 k points for tantalum.

	14 k points E (Ry)	Δ_E (mRy)	55 k points E (Ry)	Δ_E (mRy)	5 k points E (Ry)
Γ_1	−0.635 18	1.3	−0.633 92	−11.6	−0.646 76
N_1	−0.382 22	0.8	−0.381 42	−7.5	−0.389 75
H_{12}	−0.357 52	0.7	−0.356 84	−6.5	−0.364 03
N_2	−0.167 44	0.3	−0.167 15	−2.8	−0.170 19
P_4	−0.149 05	0.6	−0.148 46	−5.3	−0.154 36
Γ'_{25}	0.000 00	0.0	0.000 00	0.0	0.000 00
N'_1	0.052 29	1.2	0.053 47	−10.6	0.041 67
Γ_{12}	0.209 26	−0.1	0.209 15	1.0	0.210 27
N_1	0.213 63	−0.2	0.213 48	1.5	0.215 11

TABLE III. Comparison between relativistic and nonrelativistic calculations, iterating with 14 k points, for chromium and molybdenum.

	Chromium			Molybdenum		
	Relat. E (Ry)	Δ_E (mRy)	Nonrelat. E (Ry)	Relat. E (Ry)	Δ_E (mRy)	Nonrelat. E (Ry)
Γ_1	−0.512 60	28.9	−0.483 70	−0.443 76	74.1	−0.369 71
Γ_{12}	0.132 65	−2.0	0.130 65	0.198 91	−3.1	0.195 80
Γ'_{25}	0.000 00	0.0	0.000 00	0.000 00	0.0	0.000 00
N_1	−0.257 43	9.9	−0.247 51	−0.302 61	21.6	−0.281 04
N'_1	0.130 59	17.2	0.147 79	0.204 63	39.2	0.243 80
N_2	0.108 74	2.1	−0.106 66	−0.150 90	3.5	−0.147 41
N_3	0.260 26	−4.6	0.255 66	0.440 16	−10.1	0.430 09
N_4	0.159 70	−2.8	0.156 87	0.254 42	−5.5	0.248 95
P_1				0.805 09	93.0	0.898 13
P_3	0.163 89	−2.9	0.160 98	0.263 44	−5.9	0.257 56
P_4	0.103 78	5.4	−0.098 39	−0.098 23	12.5	−0.085 74
H_{12}	0.255 18	5.0	−0.250 17	−0.323 76	7.7	−0.316 05
H'_{25}	0.231 85	−4.1	0.227 80	0.382 77	−8.4	0.374 39
H_{15}	0.822 23	18.0	0.840 21	0.768 77	38.0	0.806 80
$H'_{25}-\Gamma_1$	0.744 45	−32.9	0.711 50	0.826 53	−82.4	0.744 10
$H'_{25}-H_{12}$	0.487 03	−9.1	0.477 97	0.706 53	−16.1	0.690 44
$N'_1-\Gamma_1$	0.643 19	−11.7	0.631 49	0.648 39	−34.9	0.613 51
E_F	0.063 49	0.4	0.063 88	0.095 06	6.1	0.101 21
E_F-H_{12}	0.318 67	−4.6	0.314 05	0.418 82	−1.6	0.417 26
$E_F-\Gamma_1$	0.576 09	−28.5	0.547 58	0.538 82	−67.9	0.470 92
			DOS at E_F (states/Ry cell)			
	9.782 89		10.389 43	7.996 08		9.193 08

TABLE IV. Comparison between the frozen-core and the soft-core approximations for chromium, molybdenum, and tungsten. Iterations with 14 k points. Relativistic calculation.

	Vanadium			Niobium			Tantalum		
	Soft core E (Ry)	Δ_E (mRy)	Frozen core E (Ry)	Soft core E (Ry)	Δ_E (mRy)	Frozen core E (Ry)	Soft core E (Ry)	Δ_E (mRy)	Frozen core E (Ry)
Γ_1	−0.510 57	−6.3	−0.516 89	−0.469 62	−3.0	−0.472 65	−0.669 57	−6.0	−0.6755
Γ_{12}	0.130 08	0.8	0.130 92	0.189 42	0.3	0.189 73	0.209 25	0.8	0.2100
Γ'_{25}	0.000 00	0.0	0.000 00	0.000 00	0.0	0.000 00	0.000 00	0.0	0.000 00
N_1	−0.261 81	−3.5	−0.265 32	−0.310 23	−1.9	−0.312 08	−0.393 68	−4.3	−0.3980
N'_1	0.081 88	−5.9	0.076 00	0.131 91	−2.7	0.129 21	0.057 92	−4.7	0.0532
N_2	−0.109 14	−1.2	−0.110 30	−0.149 87	−0.7	−0.150 59	−0.167 39	−1.7	−0.1691
N_1	0.259 34	2.1	0.261 47	0.433 17	1.6	0.434 78	0.504 48	4.6	0.5090
N_4	0.158 86	1.3	0.160 18	0.249 06	0.8	0.249 89	0.284 27	2.3	0.2865
N'_4				0.803 97	−3.4	0.800 58	0.785 55	−6.8	0.7787
P_1	0.824 76	−5.2	0.819 58	0.673 34	−2.2	0.671 17	0.427 68	−3.4	0.4242
P_1	0.163 30	1.4	0.164 67	0.258 70	0.9	0.259 65	0.296 70	2.6	0.2992
P_4	−0.110 94	−2.4	−0.113 32	−0.111 60	−1.2	−0.112 83	−0.147 07	−2.6	−0.1496
H_{12}	−0.257 10	−3.0	−0.260 07	−0.323 94	−1.7	−0.325 66	−0.357 40	−4.0	−0.3613
H'_{25}	0.230 67	1.9	0.232 54	0.375 28	1.3	0.376 60	0.432 76	3.6	0.4363
H_{15}	0.711 70	−5.6	0.706 06	0.647 05	−2.6	0.644 48	0.590 71	−4.4	0.5863
$H'_{25}-\Gamma_1$	0.741 24	8.2	0.749 43	0.844 90	4.4	0.849 25	1.102 33	9.6	1.1119
$H'_{25}-H_{12}$	0.487 77	4.8	0.492 61	0.699 22	3.0	0.702 26	0.790 16	7.6	0.7977
$N'_1-\Gamma_1$	0.592 45	0.4	0.592 89	0.601 53	0.3	0.601 86	0.727 49	1.3	0.7287
E_F	−0.031 65	−1.3	−0.032 94	−0.032 44	4.3	−0.028 11	−0.059 17	−2.0	−0.0611
E_F-H_{12}	0.225 45	1.7	0.227 13	0.291 50	6.0	0.297 55	0.298 23	2.0	0.3002
$E_F-\Gamma_1$	0.478 92	5.0	0.483 95	0.437 18	7.4	0.444 54	0.610 40	4.0	0.6143
				DOS at E_F (states/Ry cell)					
	29.787 02		29.059 99	23.699 86		20.913 45	20.754 21		20.4688

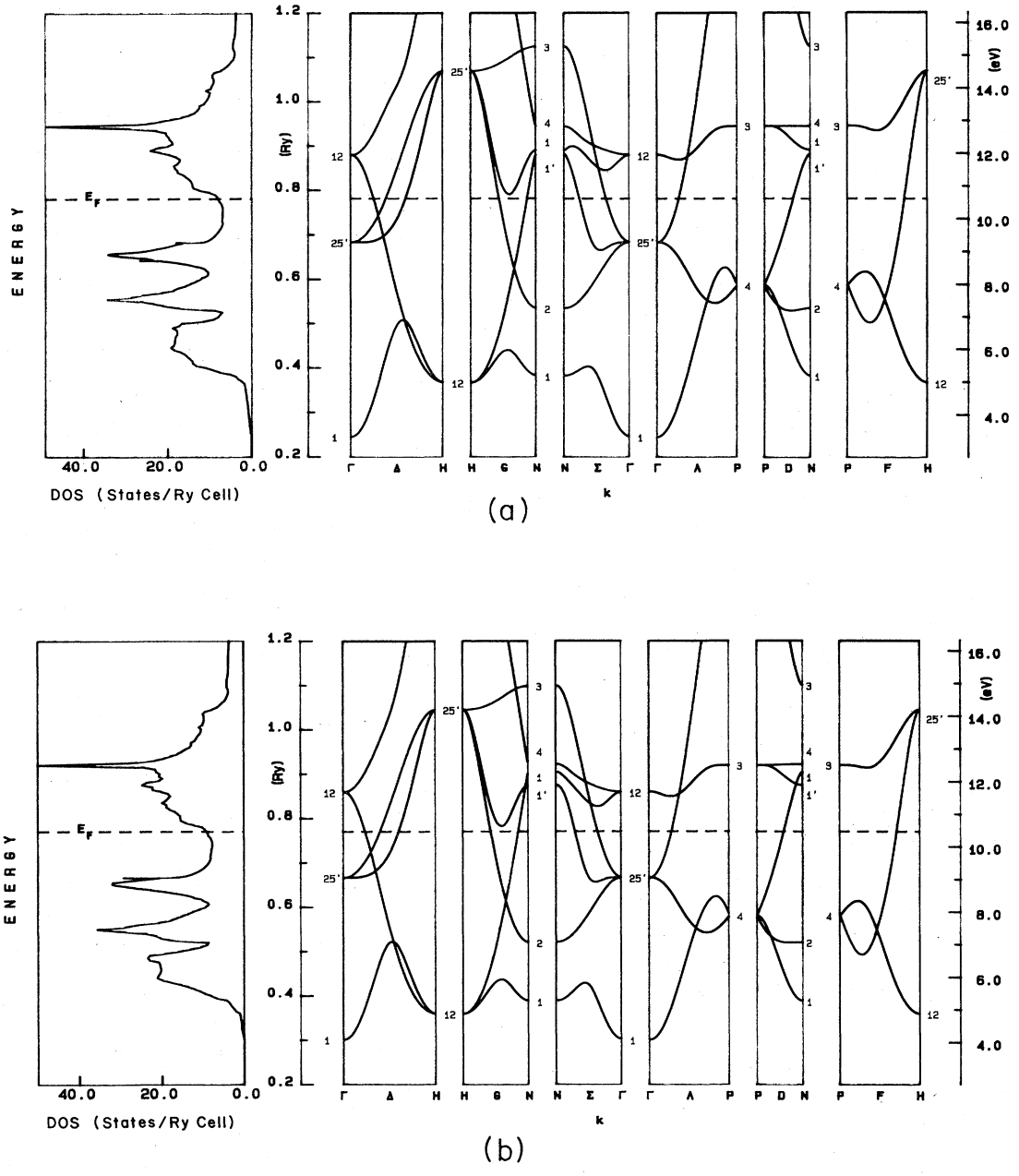

FIG. 1. Band structure and density of states of molybdenum. (a) Relativistic calculation, (b) nonrelativistic calculation.

separation ($H'_{25}-\Gamma_1$) is affected the most by the relativistic effects, the differences being 2–3 times larger than those of the *s-p* separation ($N'_1-\Gamma_1$). $H'_{25}-\Gamma_1$ increases by 17.3 mRy and $N'_1-\Gamma_1$ by 3.9 mRy for V. For the other elements these separations are, respectively, 33.9 and 7.5 mRy for Nb, 32.9 and 11.7 mRy for Cr, and 82.4 and 34.9 mRy for Mo. The *d*-band width $H'_{25}-H_{12}$ is most affected for Nb and Mo (it increases by 30.9 and 16.1 mRy, respectively) and less for V and Cr (increasing by 5.0 and 9.1 mRy, respectively). The energies which are most affected by the relativistic effects are at the symmetry points Γ_1, N'_1, N'_4, P_1, and H_{15}. Thus, the *d* states are affected the least.

C. Comparison between the frozen-core and soft-core approximations

The differences between the energy calculated using the frozen-core and that using the soft-core approximations have an average deviation of 3.1, 1.7, and 3.7 mRy for V, Nb, and Ta, respectively. We note from Table IV that the *s* states are affected the most, and that the *d* states are affected the least.

TABLE V. Comparison between the semicore and the soft-core approximations for vanadium, niobium, and tantalum. Iterations with 14 k points. Relativistic calculation.

	Vanadium			Niobium			Tantalum		
	Soft core E (Ry)	Δ_E (mRy)	Semicore E (Ry)	Soft core E (Ry)	Δ_E (mRy)	Semicore E (Ry)	Soft core E (Ry)	Δ_E (mRy)	Semicore E (Ry)
Γ_1	−0.510 57	−5.4	−0.515 93	−0.469 62	0.8	−0.468 77	−0.669 57	0.9	−0.668 68
Γ_{12}	0.130 08	0.0	0.130 05	0.189 42	0.1	0.189 53	0.209 25	−0.1	0.209 20
Γ'_{25}	0.000 00	0.0	0.000 00	0.000 00	0.0	0.000 00	0.000 00	0.0	0.000 00
N_1	−0.261 81	−1.1	−0.262 89	−0.310 23	0.6	−0.309 66	−0.393 68	0.7	−0.392 97
N'_1	0.081 88	0.6	0.082 48	0.131 91	0.9	0.132 80	0.057 92	0.5	0.058 42
N_2	−0.109 14	0.1	−0.109 05	−0.149 87	0.2	−0.149 67	−0.167 39	0.3	−0.167 09
N_3	0.259 34	−0.1	0.259 19	0.433 17	−0.2	0.433 00	0.504 48	−0.7	0.503 74
N_4	0.158 86	−0.1	0.158 77	0.249 06	−0.1	0.248 96	0.284 27	−0.3	0.283 94
N'_4				0.803 97	1.2	0.805 19	0.785 55	1.2	0.786 74
P_1	0.824 76	−6.4	0.818 39	0.673 34	0.1	0.673 44	0.427 68	0.5	0.428 16
P_3	0.163 30	−0.1	0.163 19	0.258 70	−0.1	0.258 59	0.296 70	−0.4	0.296 30
P_4	−0.110 94	0.2	−0.110 71	−0.111 60	0.4	−0.111 19	−0.147 07	0.3	−0.146 72
H_{12}	−0.257 10	0.3	−0.256 82	−0.323 94	0.7	−0.323 27	−0.357 40	0.8	−0.356 64
H'_{25}	0.230 67	−0.1	0.230 55	0.375 28	−0.2	0.375 11	0.432 76	−0.6	0.432 14
H_{15}	0.711 70	0.6	0.712 32	0.647 05	0.5	0.647 59	0.590 71	0.4	0.591 09
$H'_{25}-\Gamma_1$	0.741 24	5.2	0.746 48	0.844 90	−1.0	0.843 88	1.102 33	−1.5	1.100 82
$H'_{25}-H_{12}$	0.487 77	−0.4	0.487 37	0.699 22	−0.8	0.698 38	0.790 16	−1.4	0.788 78
$N'_1-\Gamma_1$	0.592 45	6.0	0.598 41	0.601 53	0.0	0.601 57	0.727 49	−0.4	0.727 10
E_F	−0.031 65	0.2	−0.031 48	−0.032 44	0.1	−0.032 36	−0.059 17	0.5	−0.058 66
E_F-H_{12}	0.225 45	−0.1	0.225 34	0.291 50	−0.6	0.290 91	0.298 23	−0.2	0.297 98
$E_F-\Gamma_1$	0.478 92	5.5	0.484 45	0.437 18	−0.8	0.436 41	0.610 40	−0.4	0.610 02
				DOS at E_F (states/Ry cell)					
	29.787 02		29.722 57	23.699 86		23.928 83	20.754 21		20.736 42

D. Comparison between the semicore and soft-core approximations

As seen from Table V, the differences between the results using the semicore approximation and those using the soft-core are even smaller than those found in the frozen-semicore comparison. The average deviations are 1.2, 0.4, and 1.2 mRy for V, Nb, and Ta, respectively. The s states are again affected the most and the d states are affected the least. It should be mentioned here that in the relativistic calculations the core levels are calculated including the spin-orbit coupling, whereas in the valence bands and the semi-core states the spin-orbit interaction is omitted. This is important for heavier elements but not for lighter elements. On the other hand, the crystal-field splittings incorporated by treating the levels as bands are equally important for all elements. Thus, the semicore approximation is probably better than the soft-core for light elements where the spin-orbit interaction is weak. However, the soft-core approximation, which includes the spin-orbit interaction, in the core levels, might be better than the semicore for heavier elements.

E. Spin-orbit coupling corrections

The spin-orbit Hamiltonian has the form

$$H_{\mathrm{SO}}=\xi \mathbf{l}\cdot\mathbf{s} .$$

We calculated the spin-orbit parameter ξ as a function of the k point and its energy for each k point which is split. In an obvious generalization of the atomic expression, we used, to first order in perturbation theory, the formula

$$\xi_l=\frac{\alpha^2}{2}\int_0^R \frac{1}{r}\frac{\partial V}{\partial r}R_l^2 r^2 dr ,$$

where l is the angular momentum which contributes to the k point by an amount Q_l. Q_l is the electronic charge inside the APW sphere and α is the fine-structure constant. $V(r)$ is the crystal potential and $R_l(r)$ is the lth radial wave function for the particular k point. $V(r)$ and $R_l(r)$ were extrapolated outside the muffin-tin sphere out to a point R so that the potential at the radius R would have the same value as the constant interstitial potential employed in the muffin-tin approximation. We decided on this prescription for the extrapolation because we used it to calculate the Darwin correction and the mass-velocity correction to nonrelativistic APW calculations, again by first-order perturbation theory. The results agree to within 1 mRy with the relativistic energies (excluding spin-orbit coupling) that we find when we solve Dirac's equation.

The results for the elements we studied are shown in Tables VI and VII. These tables show the k points with their degeneracies and their energies (in Ry) with respect

TABLE VI. Spin-orbit splitting parameter ξ_l and fractional charge Q_l for vanadium, niobium, and tantalum.

	Degen.	E (Ry)	ξ_p (mRy)	Q_p	ξ_d (mRy)	Q_d
			Vanadium			
$\Gamma'_{25}(000)$	3	0.000 00	0.0	0.00	2.0	0.96
$P_4(444)$	3	−0.110 82	14.5	0.13	1.7	0.68
$P_4(444)$	3	0.707 60	15.2	0.26	3.4	0.43
$H'_{25}(800)$	3	0.230 60	0.0	0.00	2.7	0.99
$H_{15}(800)$	3	0.712 21	15.2	0.58	0.0	0.00
$\Delta_5(200)$	2	−0.001 24	14.4	0.01	2.0	0.93
$\Delta_5(200)$	2	1.484 71	17.8	0.06	2.7	0.21
$\Delta_5(400)$	2	0.031 27	14.4	0.04	2.1	0.88
$\Delta_5(400)$	2	1.239 46	16.8	0.36	3.0	0.31
$\Delta_5(600)$	2	0.136 83	14.5	0.05	2.4	0.88
$\Delta_5(600)$	2	0.896 10	15.7	0.49	3.3	0.16
$\Lambda_3(222)$	2	−0.083 01	14.5	0.02	1.8	0.86
$\Lambda_3(222)$	2	0.134 95	14.5	0.00	2.4	0.96
$\Lambda_3(222)$	2	1.116 95	16.4	0.18	3.1	0.31
			Niobium			
$\Gamma'_{25}(000)$	3	0.000 00	0.0	0.00	5.8	0.92
$P_4(444)$	3	−0.111 62	64.8	0.16	5.0	0.60
$P_4(444)$	3	0.831 38	62.4	0.20	12.0	0.41
$H'_{25}(800)$	3	0.375 27	0.0	0.00	8.8	0.97
$H_{15}(800)$	3	0.647 04	61.8	0.50	0.0	0.00
$\Delta_5(200)$	2	−0.003 43	63.7	0.02	5.8	0.87
$\Delta_5(200)$	2	1.156 39	64.7	0.00	13.0	0.07
$\Delta_5(400$	2	0.042 82	63.3	0.06	6.1	0.79
$\Delta_5(400)$	2	1.311 51	66.2	0.24	13.0	0.33
$\Delta_5(600)$	2	0.197 07	62.3	0.09	7.3	0.75
$\Delta_5(600)$	2	0.929 14	63.0	0.39	12.4	0.25
$\Lambda_3(222)$	2	−0.112 10	64.8	0.03	5.0	0.79
$\Lambda_3(222)$	2	0.200 33	62.3	0.00	7.3	0.91
$\Lambda_3(222)$	2	1.078 70	64.0	0.13	12.8	0.25
			Tantalum			
$\Gamma'_{25}(000)$	3	0.000 00	0.0	0.00	21.3	0.91
$P_4(444)$	3	−0.147 09	251.1	0.17	17.8	0.56
$P_4(444)$	3	0.864 53	261.9	0.19	45.7	0.44
$H'_{25}(800)$	3	0.432 74	0.0	0.00	33.9	0.96
$H_{15}(800)$	3	0.590 70	253.0	0.51	0.0	0.00
$\Delta_5(200)$	2	−0.006 61	248.6	0.02	21.1	0.85
$\Delta_5(200)$	2	1.175 17	276.5	0.00	50.1	0.06
$\Delta_5(400)$	2	0.037 98	248.1	0.07	22.3	0.75
$\Delta_5(400)$	2	1.356 59	287.2	0.27	50.8	0.34
$\Delta_5(600$	2	0.203 09	247.6	0.12	26.9	0.68
$\Delta_5(600)$	2	0.932 90	264.7	0.38	47.0	0.30
$\Lambda_3(222)$	2	−0.130 38	250.7	0.04	18.1	0.76
$\Lambda_3(222)$	2	0.224 97	247.7	0.00	27.5	0.89
$\Lambda_3(222)$	2	1.107 45	273.0	0.14	49.4	0.25

to Γ'_{25}. The ξ_l's are also shown in mRy together with the Q_l's inside the muffin-tin spheres.

As can be seen and expected from the tables, the spin-orbit parameter ξ increases with the mass of the element. ξ varies to within a factor of 2 for different energies and k points. The largest for each element is for H_{15}, generally an order of magnitude larger than the others. Mattheiss and Hamann,[7] using a tight-binding fit to their APW results for W, estimated average values for $\xi_{5d}=26$ mRy and $\xi_{6p}=126$ mRy. Our first-order perturbation-theory results yield the values $\xi_{5d}=33$ mRy and $\xi_{6p}=290$ mRy. The estimated splittings are generally a factor of 2 larger than in the free atoms.[8] The free-atom splittings for Cr $3d$, Mo $4d$, and W $5d$ are 1.4, 3.7, and 13.7 mRy, respectively, which, as in the solid, increase with the mass of the element.

TABLE VII. Spin-orbit splitting parameter ξ_l and fractional charge Q_l for chromium, molybdenum, and tungsten.

	Degen.	E (Ry)	ξ_p (mRy)	Q_p	ξ_d (mRy)	Q_d
			Chromium			
$\Gamma'_{25}(000)$	3	0.000 00	0.0	0.00	2.7	0.96
$P_4(444)$	3	−0.103 76	16.1	0.12	2.3	0.71
$P_4(444)$	3	0.781 45	17.4	0.28	4.3	0.40
$H'_{25}(800)$	3	0.231 85	0.0	0.00	3.5	0.99
$H_{15}(800)$	3	0.822 23	17.5	0.58	0.0	0.00
$\Delta_5(200)$	2	0.000 13	16.1	0.01	2.7	0.93
$\Delta_5(200)$	2	1.671 34	21.0	0.07	3.2	0.23
$\Delta_5(400)$	2	0.035 36	16.2	0.03	2.8	0.89
$\Delta_5(400)$	2	1.376 72	19.6	0.36	3.6	0.30
$\Delta_5(600)$	2	0.142 45	16.2	0.04	3.2	0.90
$\Delta_5(600)$	2	1.009 35	18.1	0.50	4.1	0.15
$\Lambda_3(222)$	2	−0.080 28	16.1	0.02	2.4	0.87
$\Lambda_3(222)$	2	0.136 90	16.2	0.00	3.2	0.96
$\Lambda_3(222)$	2	1.248 45	19.0	0.18	3.8	0.31
			Molybdenum			
$\Gamma'_{25}(000)$	3	0.000 00	0.0	0.00	7.1	0.93
$P_4(444)$	3	−0.098 22	66.7	0.14	6.3	0.64
$P_4(444)$	3	0.926 08	66.8	0.22	14.5	0.39
$H'_{25}(800)$	3	0.382 77	0.0	0.00	10.7	0.97
$H_{15}(800)$	3	0.768 79	65.8	0.50	0.0	0.00
$\Delta_5(200)$	2	−0.000 16	66.0	0.01	7.1	0.88
$\Delta_5(200)$	2	1.324 38	70.6	0.00	14.9	0.07
$\Delta_5(400)$	2	0.052 92	65.7	0.05	7.6	0.81
$\Delta_5(400)$	2	1.458 43	72.3	0.25	14.7	0.31
$\Delta_5(600)$	2	0.214 97	65.0	0.07	9.1	0.79
$\Delta_5(600)$	2	1.048 55	67.8	0.40	14.8	0.22
$\Lambda_3(222)$	2	−0.107 75	66.8	0.03	6.2	0.81
$\Lambda_3(222)$	2	0.208 20	65.0	0.00	9.0	0.92
$\Lambda_3(222)$	2	1.216 18	69.4	0.13	15.0	0.24
			Tungsten			
$\Gamma'_{25}(000)$	3	0.000 00	0.0	0.00	25.5	0.92
$P_4(444)$	3	−0.131 51	289.7	0.16	22.1	0.59
$P_4(444)$	3	0.968 34	298.7	0.20	54.0	0.41
$H'_{25}(800)$	3	0.456 71	0.0	0.00	39.7	0.96
$H_{15}(800)$	3	0.709 84	290.5	0.50	0.0	0.00
$\Delta_5(200)$	2	−0.003 28	286.8	0.02	25.4	0.86
$\Delta_5(200)$	2	1.319 14	314.9	0.00	58.3	0.06
$\Delta_5(400)$	2	0.050 77	286.0	0.06	27.0	0.77
$\Delta_5(400)$	2	1.515 12	326.3	0.26	58.8	0.32
$\Delta_5(600)$	2	0.231 74	284.6	0.10	32.4	0.72
$\Delta_5(600)$	2	1.057 67	302.2	0.39	55.6	0.27
$\Lambda_3(222)$	2	−0.128 94	289.6	0.03	22.1	0.78
$\Lambda_3(222)$	2	0.240 51	284.6	0.00	32.7	0.90
$\Lambda_3(222)$	2	1.242 31	310.8	0.14	57.8	0.24

IV. APPLICATION TO THE ELECTRON-PHONON INTERACTION

In order to check the effect of the approximation discussed in the present work on a quantity with physical significance, we calculated the electron-phonon interaction η, using the theory of Gaspari and Gyorffy.[9] In this theory, η is evaluated in terms of the partial DOS at E_F and the scattering phase shifts found from the APW po-

TABLE VIII. Electron-phonon interaction parameter η.

	η (eV/Å^2)	
	Soft core	Frozen core
V	8.67	8.61
Nb	9.77	10.92
Ta	9.74	9.82
Cr	3.99	4.00
Mo	5.33	5.32
W	5.01	5.16

tentials. Our results, which correspond to DOS generated from 55 first-principles k points, are summarized in Table VIII. It is clear that the difference in η for the various approximations examined here is not significant.

V. SUMMARY AND CONCLUSIONS

We studied the relativistic effects, the soft-core approximation, the frozen-core approximation, and the semicore approximation for the band structures of the elements V, Nb, Ta, Cr, Mo, and W, as well as the convergence with different k-point meshes. The relativistic effects increase with the mass of the atom, and they are more pronounced for s and p states. This holds also for the spin-orbit coupling which was studied separately. The frozen-core approximation introduces an average deviation of approximately 3 mRy from the soft-core approach. The semicore approximation introduces a smaller change but it raises the point that for the heavy elements, due to the inclusion of the spin-orbit coupling in the core states, the soft-core approach may be more appropriate. Concerning the number of k points in the meshes, 14 k points are practically enough for satisfactory accuracy in the determination of the self-consistent potential. However, it is certainly inadequate for the calculation of the density of states for which even 55 k points do not produce a well-converged DOS. We found that it is necessary to use a 285-k-point mesh in the calculation of the density of states to achieve satisfactory accuracy. Finally, we pointed out that first-order perturbation theory seems to give a good account of the spin-orbit splitting at high-symmetry points.

[1]L. F. Mattheiss, J. H. Wood, and A. C. Switendick, Methods Comput. Phys. **8**, 63 (1968).

[2]See, for example, D. A. Papaconstantopolous, J. R. Anderson, and J. W. McCaffrey, Phys. Rev. B **5**, 1214 (1972); J. R. Anderson, D. A. Papaconstantopoulos, J. W. McCaffrey, and J E. Schirber, *ibid.* **7**, 5115 (1973); L. L. Boyer, D. A. Papaconstantopoulos, and B. M. Klein, *ibid.* **15**, 3685 (1977).

[3]R. W. G. Wyckoff, *Crystal Structures* (Interscience, New York, 1963).

[4]L. Hedin and B. I. Lundqvist, J. Phys. C **4**, 2064 (1971).

[5]G. Lehman and M. Taut, Phys. Status Solidi B **54**, 469 (1972); O. Jepsen and O. K. Anderson, Solid State Commun. **9**, 1763 (1971); Phys. Rev. B **29**, 5965 (1984); L. Kleinman, *ibid.* **28**, 1139 (1983).

[6]K. Schwarz, Phys. Rev. B **5**, 2466 (1972).

[7]L. F. Mattheiss and D. R. Hamann, Phys. Rev. B **29**, 5372 (1984).

[8]F. Herman and S. Skillman, *Atomic Structure Calculations* (Prentice-Hall, Englewood Cliffs, NJ, 1963).

[9]G. D. Gaspari and B. L. Gyorffy, Phys. Rev. Lett. **28**, 801 (1972).